The Plant Journal (2002) **32**, 495–508

Loss-of-function of a rice brassinosteroid biosynthetic enzyme, C-6 oxidase, prevents the organized arrangement and polar elongation of cells in the leaves and stem

Zhi Hong[1], Miyako Ueguchi-Tanaka[1], Sae Shimizu-Sato[1], Yoshiaki Inukai[1], Shozo Fujioka[2], Yukihisa Shimada[2], Suguru Takatsuto[3], Masakazu Agetsuma[1], Shigeo Yoshida[2], Yoshihisa Watanabe[4], Sakurako Uozu[4], Hidemi Kitano[4], Motoyuki Ashikari[1], Makoto Matsuoka[1,*]

[1]*BioScience Center, Nagoya University, Chikusa, Nagoya 464-8601, Japan*
[2]*RIKEN (The Institute of Physical and Chemical Research), Wako-shi, Saitama 351-0198, Japan*
[3]*Department of Chemistry, Joetsu University of Education, Joetsu-shi, Niigata 943-8512, Japan, and*
[4]*Graduate School of Bioagricultural Sciences, Nagoya University, Chikusa, Nagoya 464-8601, Japan*

Received 11 May 2002; revised 24 June 2002; accepted 17 July 2002.
*For correspondence (fax: +81 52 789 5226; e-mail: makoto@nuagr1.agr.nagoya-u.ac.jp).

Summary

Molecular genetic and physiological studies on brassinosteroid (BR)-related mutants of dicot plants have revealed that BRs play important roles in normal plant growth and development. However, little is known about the function of BR in monocots (grasses), except for the phenotypic analysis of a rice mutant partially insensitive to BR signaling. To investigate the function of BR in monocots, we identified and characterized BR-deficient mutants of rice, *BR-deficient dwarf1* (*brd1*). The *brd1* mutants showed a range of abnormalities in organ development and growth, the most striking of which were defects in the elongation of the stem and leaves. Light microscopic observations revealed that this abnormality was primarily owing to a failure in the organization and polar elongation of the leaf and stem cells. The accumulation profile of BR compounds in the *brd1* mutants suggested that these plants may be deficient in the activity of BR C-6 oxidase. Therefore, we cloned a rice gene, *OsDWARF*, which has a high sequence similarity to the tomato C-6 oxidase gene, *DWARF*. Introduction of the wild-type *OsDWARF* gene into *brd1* rescued the abnormal phenotype of the mutants. The *OsDWARF* gene was expressed at a low level in all of the examined tissues, with preferential expression in the leaf sheath, and the expression was negatively regulated by brassinolide treatment. On the basis of these findings, we discuss the biological function of BRs in rice plants.

Keywords: brassinosteroid, cell elongation, cytochrome P450, dwarf, rice.

Introduction

Many dwarf mutants of rice have been identified and characterized, because rice varieties with a semi-dwarf phenotype improve grain yield owing to their reduced straw biomass and increased resistance to wind and rain damage (Evans, 1993; Gale and Youssefian, 1985). Various factors cause the dwarf phenotype in plants, but the most investigated factor for determining the height of rice plants is gibberellin (GA). To date, we have screened and characterized several rice GA-related mutants and isolated the genes involved in GA biosynthesis and signal transduction (Ashikari *et al.*, 1999; Itoh *et al.*, 2001; 2002; Sasaki *et al.*, 2002; Ueguchi-Tanaka *et al.*, 2000).

Recent molecular genetic approaches have revealed that brassinosteroids (BRs) are another important factor for determining plant height. In *Arabidopsis*, for example, a number of mutants mapping to different loci have been identified as BR-related mutants with distinctive dwarf phenotype. These BR-related mutants also have defects in dark-adapted morphogenesis (skotomorphogenesis), including the elongation in darkness of the hypocotyl and closed cotyledons. Detailed anatomical analyses of the *Arabidopsis* BR-deficient mutants *det2* and *dwf1* have revealed that BRs have an important role in cell elongation and proliferation (Nakaya *et al.*, 2002). This has also been

supported by BR-application experiments (Sasse, 1999). Consequently, BRs are considered to be important for the normal development of dicot plants.

In contrast to the dicots, studies on the role of BRs in monocot plants have been limited to some physiological observations. The stimulation of lamina inclination in rice is one of the most well-known effects of BRs in monocots, and has been used for a sensitivity bioassay of BRs (Maeda, 1965; Takeno and Pharis, 1982; Wada *et al.*, 1981). In addition, treatment of etiolated wheat seedlings with brassinolide (BL) has been shown to stimulate the unrolling of leaf blades (Wada *et al.*, 1985). These BR-application experiments have demonstrated that exogenously applied BRs affect the growth and developmental processes of grass plants. Therefore, as is the case for dicots, endogenous BRs may also be important for normal growth and development in monocot plants.

Recently, we characterized a rice dwarf mutant, *d61*, that shows a distinctive dwarf phenotype with erect leaves. We reported that the *d61* mutation is caused by the loss-of-function of the *OsBRI1* gene, which encodes a putative protein kinase highly similar to the *Arabidopsis* BRI1 protein, a putative BR receptor in *Arabidopsis* (Yamamuro *et al.*, 2000). The *d61* mutant served as a cue to investigate the functional role of BRs in grass plants. In fact, the phenotypic analyses of the *d61* mutants indicated that BRs may be important for internode elongation, bending of the lamina joint, and skotomorphogenesis. The mutants used in analyses were weak, and consequently the predicted biological roles of BRs in monocot plants could only be predicted by the partial and/or weak phenotypes of the mutants. Therefore, we set out to identify rice BR-related mutants with a severe phenotype in order to further investigate the biological role of BRs in rice plants.

In this study, we describe the isolation and characterization of rice BR-deficient mutants with a severe phenotype, *BR-deficient dwarf1* (*brd1*). Molecular genetic studies revealed that the loss-of-function of a gene (*OsDWARF*), encoding a protein homologous to the tomato and *Arabidopsis* DWARF proteins, which catalyze the C-6 oxidation step in BR biosynthesis (Bishop *et al.*, 1999; Shimada *et al.*, 2001), causes various abnormalities of the *brd1* mutant. Characterization of the rice *brd1* mutants demonstrated that BRs are important for leaf and stem development via the organized arrangement and polar elongation of cells in these organs.

Results

Screening of rice BR-related mutants

Based on the phenotypes of *d61* and the *OsBRI1* antisense plants (Yamamuro *et al.*, 2000), we screened more than 100 rice dwarf mutants that we have collected over many years. In screening these mutants, we used three criteria to isolate BR-related dwarf plants, that is, erect leaves, defects in skotomorphogenesis, and the ability of exogenous BL treatment to rescue the dwarf phenotype. Using these criteria, we selected 23 dwarf plants with recessive alleles as candidates for BR-related mutants. From these, we focused on one severe dwarf mutant that showed the typical BR-related dwarf phenotype. Further molecular biological studies revealed that the mutant had a loss-of-function allele of the *OsDWARF* gene encoding a protein homologous to the tomato and *Arabidopsis* DWARF proteins (see below), which catalyze the C-6 oxidation step in BR biosynthesis (Bishop *et al.*, 1999; Shimada *et al.*, 2001). In this study, we refer to this mutant as *BR-deficient dwarf1* (*brd1*). An allelism test between the *brd1* mutant and the other candidates for BR-related mutants revealed that two other dwarf mutants were allelic with *brd1*. Consequently, we named the original *brd1* mutant, *brd1-1*, and the alleles *brd1-2* and *brd1-3*.

Abnormal morphology of brd1 *mutants*

The gross morphology of the wild-type and mutant plants at 6 weeks is shown in Figure 1(a). *brd1-1* and *brd1-2* both showed a severe dwarf phenotype. These plants reached about 10 cm in height after heading, whereas the wild-type plants, Nipponbare (background cultivar of *brd1*), reached about 100 cm at the same time. The phenotype of *brd1-3* was less severe than that of the other two mutants and the plants reached a height of about 30 cm.

The *brd1* plants developed severely malformed leaves with tortuous and stiff blades (Figure 1b). Despite these abnormalities, the mutants had the normal distichous alternate phyllotaxis (Figure 1b) with the same plastochron as the wild-type plants, indicating that leaf initiation occurred normally at the shoot apical meristem (SAM). In wild-type plants, the leaf blade bends away from the vertical axis of the leaf sheath towards the abaxial side (Figure 1c), however, in the *brd1* mutants almost all of the leaves were completely erect (Figure 1d). Furthermore, although wild-type rice leaves are separated almost equally into blade and sheath by the lamina joint (indicated by the arrowhead in Figure 1c), in the mutant plants the leaf sheath was much smaller than the blade (Figure 1d). These observations indicate that the defect in BR biosynthesis affects the development of the leaf sheath more severely than the blade. However, the leaf blades of the mutants were also malformed (Figure 1d).

The defect in BR biosynthesis also affected the formation and development of a number of other organs. For example, root elongation was inhibited and the frequency of formation of crown roots was decreased in the mutants, whereas formation of lateral roots was relatively unaffected

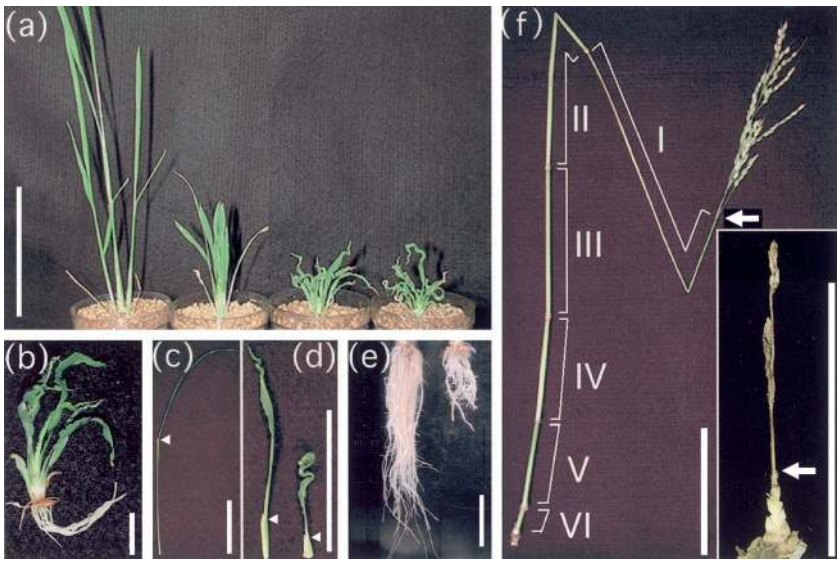

Figure 1. Morphological characterization of *brd1* mutants.
(a) Comparison of *brd1* mutants containing different alleles with the wild type. The plants were grown for 6 weeks after imbibition. From left to right: wild-type plant; *brd1-3*; *brd1-2*; and *brd1-1*. *brd1-3* had a mild phenotype, while *brd1-2* and *brd1-1* mutants showed a severe phenotype (bar: 10 cm). (b) A magnified photograph of the *brd1-1* mutant, which had the most severe phenotype (bar: 1 cm). (c, d) Leaf morphology. Arrowheads show the boundary (lamina joint) between the sheath and blade. The leaf sheath in the *brd1-3* (d, left) and *brd1-1* (d, right) mutants was shorter than in the wild-type (c) (bar: 5 cm). (e) Root morphology. The roots of the *brd1-1* mutant (right) were shorter, and crown root was less developed, than in the wild-type (left) (bar: 1 cm). (f) Culm elongation of the wild-type and *brd1-1* plants (left and right, respectively). The six uppermost internodes (I–VI) of the wild-type were elongated, whereas *brd1-1* did not have any elongated internodes. Arrows indicate the position of the boundary between the internode and neck internode (bar: 10 cm).

(Figure 1e). As we had expected, internode elongation was severely inhibited in the mutants (Figure 1f). While the uppermost five or six internodes of the wild-type plants elongated to reach about 1 m after heading, the length of the stem of *brd1-1* was about 2 cm (Figure 1f). Interestingly, elongation of the neck internode occurred even in the severe alleles of *brd1* (Figure 1f). This indicates that BRs are essential for the elongation of the internode but not for the neck internode, possibly owing to a difference in the mechanism of elongation in these regions. Internode elongation is known to be owing to the intercalary meristem, but elongation of the neck internode depends upon the rib meristem of the SAM (Yamamuro *et al.*, 2000).

Internal structures of brd1 *mutants*

The stunted culms and malformed development of the leaves of the *brd1* mutants could be caused by a defect in cell division or cell elongation, or both. To investigate these possibilities, we examined the internal structures of the unelongated internodes and malformed leaves by microscopy. Figure 2(a–e) show the cell morphology of culms in the wild-type and mutant plants. In the wild-type plants, the culm can be divided into two parts, the node and internode, on the basis of cell arrangement. Figure 2(a) shows a longitudinal section of the apical portion of the culm of a wild-type plant at the vegetative stage. At the base of each leaf primordium, the node transverses the stem with randomly arranged small cells (indicated by white arrowheads). Between two nodes, longitudinally arranged cells form an internode. During the vegetative stage, morphogenetic events cease after the differentiation of the node and internode, and no internode elongation occurs. When the SAM shifts to the reproductive phase, the uppermost five or six internodes differentiate in response to the formation of intercalary meristems in the internodes. In the intercalary meristems, active cell division occurs in an anticlinal manner to form longitudinal cell files, and longitudinal elongation of the arranged cell files also occurs (Figure 2b). The anticlinal divisions and longitudinal elongation of cells that produce the well-organized cell files (Figure 2d) are the driving force for the rapid elongation of the rice culm. In contrast to the wild-type plants, the culm of the mutant plants was not separable into nodes and internodes, even after the change from the vegetative to reproductive stage had occurred (Figure 2c). In the mutant culm, the organized longitudinal arrangement of cells that typifies the internode of wild-type plants was not observed (Figure 2e), indicating that the development of the intercalary meristem was defective. These findings demonstrate that BRs are essential for the organized arrangement of cell files in the internode.

A disorganization of the cell files also occurred in the leaf surface of the mutant plants. We observed the structure of the leaf surface of the wild-type and mutant plants by scanning electron microscopy (SEM) (Figure 2f–k). In the

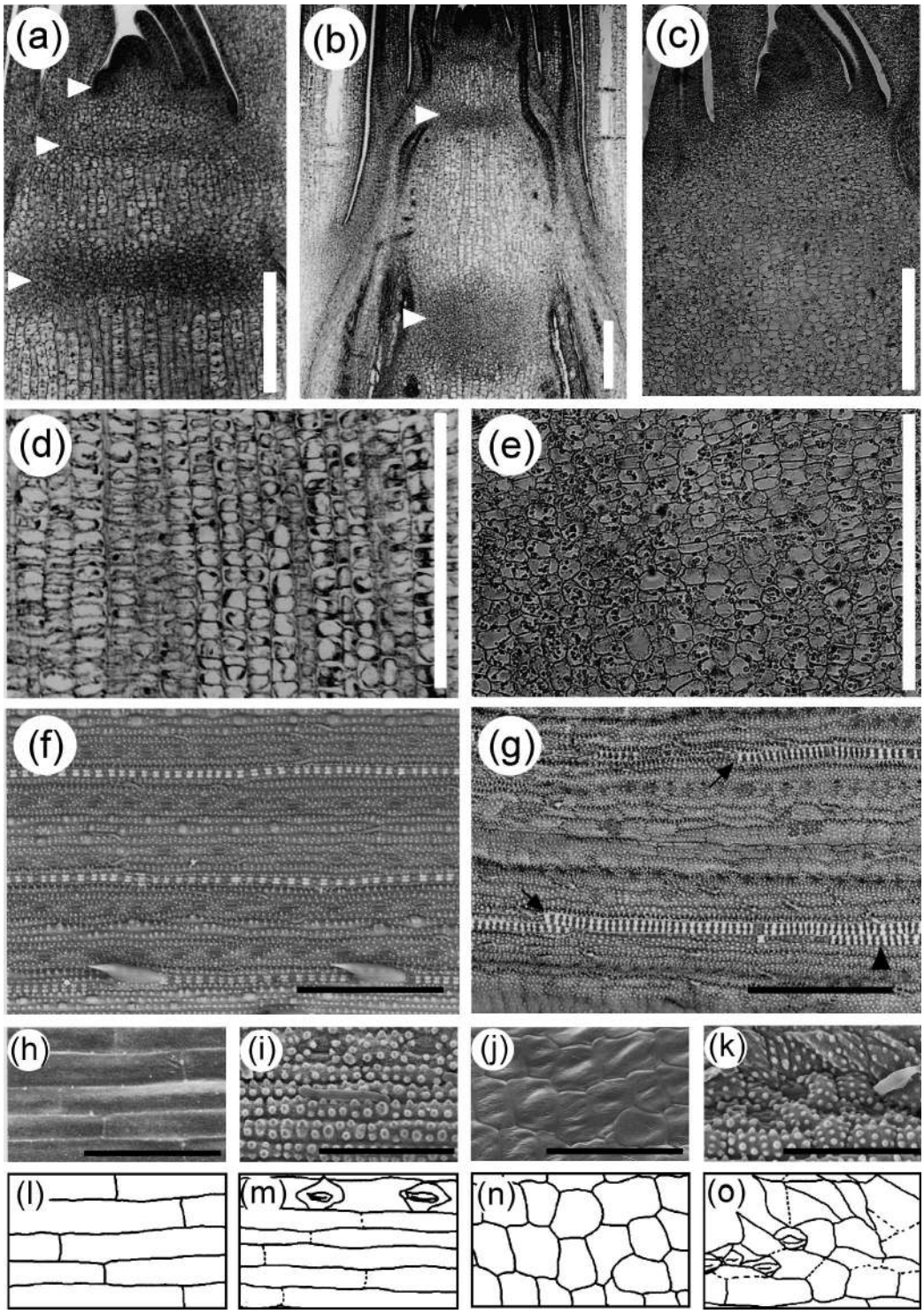

Figure 2. Microscopic observations of *brd1* mutants.
(a-c) Light micrographs of median longitudinal sections of the shoot apical region of the wild-type plants at the vegetative stage (a) or reproductive stage (b) and *brd1-1* at the reproductive stage (c). Arrowheads indicate the position of nodal region (bar: 300 μm). (d, e) Higher magnification light micrographs of the divisional zone of the intercalary meristem of the wild-type internode (d) and its corresponding region in the *brd1-1* stem (e) (bar: 300 μm). (f-k) Scanning electron micrographs of leaf surface structures of the wild-type (f, h, i) and *brd1-1* (g, j, k). The adaxial side of the leaf blade (f, g, i, k) and sheath (h, j) is shown. (g) Arrows indicate interruption of non-specialized cells on the file of dumbbell-shaped silica cells, and arrowhead indicates short fragmented files of dumbbell-shaped cells adjacent of another dumbbell-shaped cell file, respectively (bar: 200 μm in f, g; 100 μm in h–k). (l–o) Schematic representation of the leaf surface cell arrangements in the wild-type and *brd1-1* corresponding to (h–k), respectively. Lines and dashed lines indicate the clear and unclear boundary between neighboring cells, respectively.

wild-type plants, the epidermal cells of the leaf blade and sheath were arranged in a longitudinal manner running parallel to the vascular tissues (Figure 2f,h,i). However, the organized arrangement of leaf epidermal cells was disrupted in the mutants (Figure 2g,j,k). For example, the file of dumbbell-shaped silica cells was occasionally interrupted with non-specialized cells (arrows in Figure 2g), or a short fragmented file of dumbbell-shaped cells occurred adjacent to another dumbbell-shaped cell file (arrowhead in Figure 2g). These disruptions in the cell files were found in both the leaf blade and sheath of the mutants (Figure 2j,k). However, overall the organization of the leaf epidermal cells was less severely affected than the internode cells.

Scanning electron micrographs also revealed a defect in the longitudinal elongation of epidermal cells in the leaf sheath and blade of the mutant plants, as well as an abnormal expansion in a vertical direction against the cell file (for the leaf sheath, compare Figure 2h,l with Figure 2j,n; for the blade, compare Figure 2i,m with Figure 2k,o). Consequently, these cells in the mutants became round, square or otherwise distorted, whereas the wild-type cells were a uniform rectangular shape. Furthermore, the boundary between neighboring cells was more distinct in the mutants compared to the wild-type (compare Figure 2h with Figure 2j; and Figure 2i with Figure 2k). The obscure boundary of the epidermal cells of the wild-type is owing to the regular arrangement of rectangular cells covered with secretion compounds (such as silica and cuticle), whereas the irregular or spherical shape of epidermal cells in the mutants resulted in deeper grooves at the boundary of neighboring cells.

We also used light microscopy to study the internal structure of the leaf blade and sheath in transverse sections (Figure 3). Figure 3(a,b) show cross-sections through the large vascular bundle of the leaf blade in wild-type and mutant plants, respectively. In the vascular bundle of the wild-type plant, the xylem is located at the adaxial side (upper side in Figure 3a) of the phloem, and two well-developed vessels are arranged at the center and another vessel is located at the adaxial side of each vascular bundle, whereas the phloem is located at the abaxial side of the xylem. Each vascular bundle is encircled by a single layer of bundle sheath cells that contain a few chloroplasts with low chlorophyll content (Figure 3a). In contrast, vessel development was inhibited in the mutant plants, with only one fully developed vessel evident in cross sections, although the

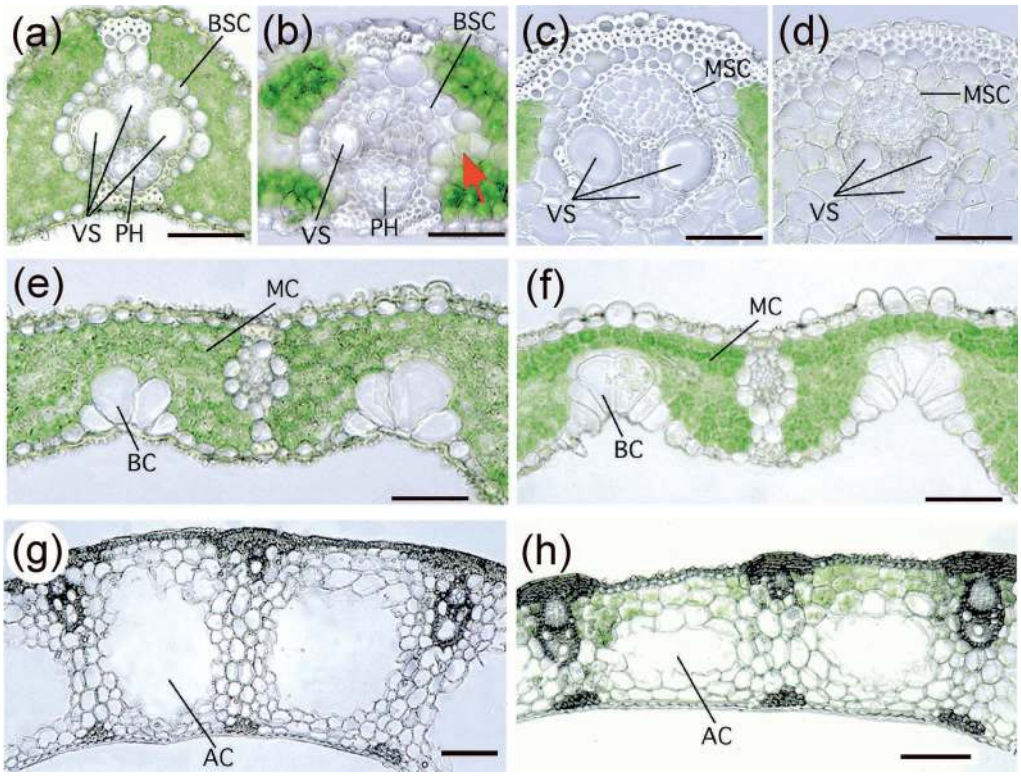

Figure 3. Internal structure of leaves in *brd1* mutants.
(a, b) Light micrographs of cross sections through the large vascular tissue of the leaf blade in the wild-type (a) and *brd1-1* (b) plants. BSC, PH, and VS indicate bundle sheath cell, phloem, and vessel, respectively. (b) Red arrow indicates abnormal arrangement of bundle sheath cells (bar: 50 μm). (c, d) Cross section of the central vascular tissue of the blade midvein in the wild-type (c) and *brd1-1* (d) plants. MSC and VS indicate the mestom sheath cell and vessel, respectively (bar: 50 μm). (e, f) Cross section of the leaf blade of the wild-type (e) and *brd1-1* (f) plants. BC and MC indicate the bulliform cells and mesophyll cells, respectively (bar: 50 μm). (g, h) Cross section of the leaf sheath of the wild-type (g) and *brd1-1* (h) plants. AC indicates aerenchyma (bar: 100 μm).

development of phloem was not affected (Figure 3b). The arrangement of the single layer of bundle sheath cells was also disturbed and enlarged cells containing few chloroplasts occurred in piles between the vascular and mesophyll cells (arrow in Figure 3b). Aberrant development of vessels and a disturbance of cell arrangement were also seen in the central vascular tissue of the midrib of the leaf blade of the mutants (compare Figure 3c for wild-type and Figure 3d for mutant). The vessel was smaller and the single layer of mestom sheath cells surrounding the phloem was disorganized. The occurrence of severe defects in vessel development is consistent with previous reports on dicot plants (Clouse and Sasse, 1998). For example, the BR-deficient *Arabidopsis* mutants *cpd* and *dwf4* developed abnormal xylem (Choe *et al.*, 1998; Szekeres *et al.*, 1996). Development of the tracheary element was promoted by exogenous treatment with BL and prevented by uniconazole, an inhibitor of BR biosynthesis (Clouse and Zurek, 1991; Iwasaki and Shibaoka, 1991). Thus, the promotion of vessel development by BRs is common in both monocot and dicot plants. Apart from the aberrant development of vascular tissue, mesophyll cells developed normally in the *brd1* mutants (Figure 3f). Interestingly, however, there were more bulliform cells in the mutants than in the wild-type plants (compare Figure 3e,f), and this may have contributed to the abnormal gross morphology of the leaf blade.

The internal structure of the leaf sheath was also examined (Figure 3g,h). The width of the leaf sheath in the mutants was less than that of the wild-type, probably because sheath development ceased at a much earlier stage in the mutants. Also, the lysigenous aerenchyma in the mutants was much smaller than in the wild-type plants.

The brd1 *mutants show a de-etiolated phenotype*

In complete darkness, *Arabidopsis* mutants that have deficiencies in BR biosynthesis or BR sensitivity show a de-etiolated (DET) phenotype characterized by less hypocotyl elongation, opening of cotyledons, and emergence of primary leaves. In a recent study, we reported that rice BR-insensitive mutants also show a DET phenotype without elongation of the mesocotyl and internode in darkness, whereas the mesocotyl and internodes of wild-type rice plants elongate to adapt to the dark conditions (Yamamuro *et al.*, 2000). To examine whether the BR-deficient mutant, *brd1-1*, also shows aberrant skotomorphogenic characteristics, we grew the mutant plants in the dark. The mesocotyl and internodes of the wild-type plants and a GA-deficient dwarf mutant, *d18*, elongated under dark conditions (Figure 4a,b, respectively), but elongation did not occur in either *brd1* (Figure 4d), or a BR-insensitive mutant, *d61* (Figure 4c). A failure in the mesocotyl or internode to elongate in the dark is not common in rice dwarf mutants, and indicates that the BR-related mutants of rice have a deficiency in skotomorphogenesis similar to that reported in *Arabidopsis* BR-related mutants.

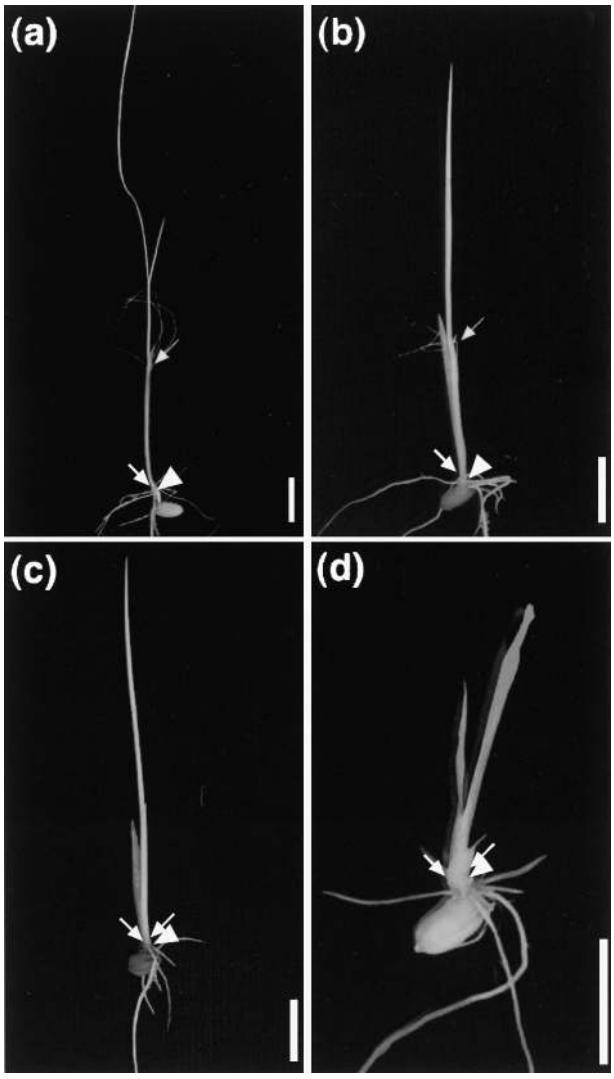

Figure 4. Aberrant skotomorphogenesis of the *brd1-1* mutant. Plants were germinated and grown in the darkness. Arrows indicate the position of nodes, and arrowheads indicate the mesocotyls. (a) wild-type; (b) GA-deficient mutant, *d18*; (c) BR-insensitive mutant, *d61*; (d) *brd1-1* (bar: 1 cm).

Quantitative analysis of BRs in brd1 *and rescue of the abnormal phenotype by BL treatment*

To confirm that BR biosynthesis was affected in the mutants, we directly measured the level of BRs in *brd1-1*, *brd1-2* and wild-type plants by gas chromatography–mass spectrometry (GC–MS) analyses. BL was not detected in the shoots of either the mutant or wild-type plants (Figure 5). Another bioactive BR, Castasterone (CS), was detected in the wild-type plants but not in the mutants. This confirms that the mutants are deficient in the biosynthesis of the

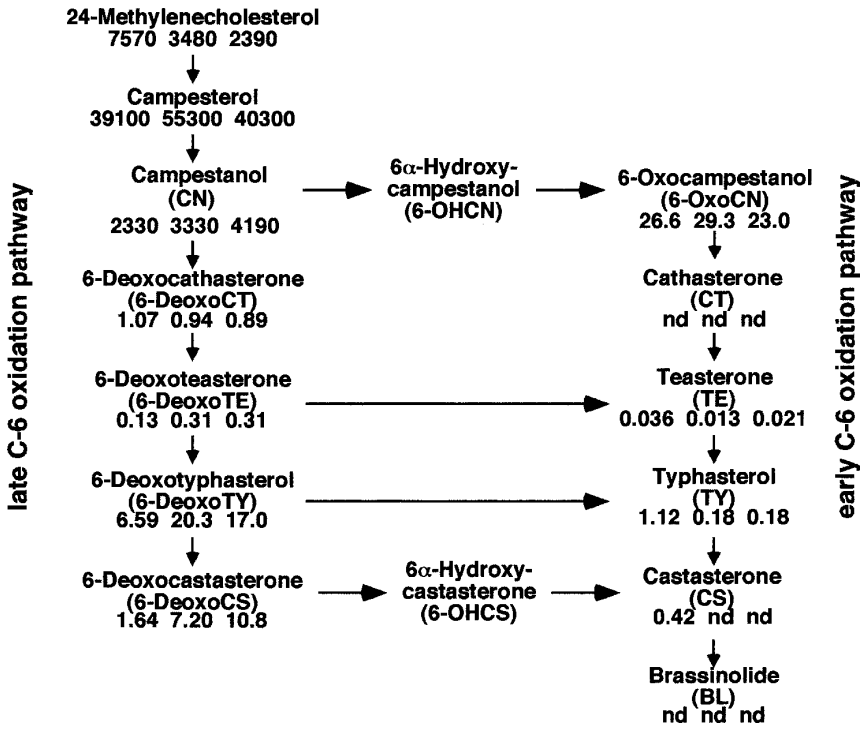

Figure 5. BR biosynthetic pathway and BR content in the wild-type, and *brd1-1* and *brd1-2* mutants. BR levels (in ng/g fresh weight) in the wild-type (left), *brd1-1* (middle), and *brd1-2* (right) are shown below each product. nd: not detected.

active BR. Interestingly, the concentration of BRs compounds in the early C-6 oxidation pathway, including CS, Typhasterol (TY) and Teasterone (TE), was much lower in the mutants than in the wild-type plants. In contrast, the level of the BR compounds in the late C-6 oxidation pathway, such as 6-Deoxocastasterone (6-DeoxoCS), 6-Deoxotyphasterol (6-DeoxoTY) and 6-Deoxotesterone (6-DeoxoTE), was increased in the mutants. The increased level of 6-Deoxo type BRs and reduced level of 6-Oxo type BRs in the mutant plants suggest that the *BRD1* gene encodes a C-6 oxidation enzyme. The fact that there was no significant difference in the levels of 6-Deoxocathasterone (6-DeoxoCT), Campestanol (CN) and 6-Oxocampestanol (6-OxoCN) detected in the mutants and wild-type plants also indicates that the BRD1 product does not catalyze the C-6 oxidation of 6-DeoxoCT or CN (see below).

We confirmed that the *brd1* mutants are deficient in active BRs by the application of BL. There was no difference between wild-type plants that had been exogenously treated with 10^{-6} M BL at the beginning of germination, and untreated plants (Figure 6). However, when the mutants were treated with BL under the same conditions, normal leaves developed and the dwarf phenotype was partially restored (Figure 6). The fact that the dwarf phenotype was only partially restored by the BL treatment may be owing to the poor incorporation of BL into the rice plants (see Discussion). Indeed, the introduction of the wild-type *BRD1* gene into the mutants completely rescued the abnormal phenotype (see below).

Cloning and characterization of the OsDWARF *gene*

The accumulation profile of BRs in the mutants suggested that the *BRD1* gene might encode a C-6 oxidase. As the gene for the C-6 oxidase of BRs from tomato, *DWARF*, has been already cloned, we searched rice EST clones with high similarity to the tomato *DWARF* gene and found one candidate clone (AU100843) likely to correspond to the *brd1* mutation. To identify the map position of *brd1*, linkage analysis was performed using the F_2 population derived from the cross between heterozygous plant for *brd1* (*brd1*/*BRD1*) and Indica variety, Kasalath. The *brd1* mutation was located on the long arm of chromosome 3 where the rice EST clone (AU100843, this EST was identical to *OsDWARF*) was co-segregated (data not shown). The result indicates that the rice EST is strong candidate for *BRD1* gene.

We isolated the full-length cDNA clone of *OsDWARF* which is corresponding to the rice EST clone (AU100843) from a cDNA library constructed using rice seed mRNA, and also isolated a genomic clone encompassing the entire region of *OsDWARF*. The longest cDNA clone was sequenced and contained a large open reading frame encoding 469 amino acid residues, a 5′-non-coding sequence of 205 nucleotides, and a 3′-non-coding sequence of 230 nucleotides without the polyA tail. The deduced amino acid sequence showed high similarity to the previously reported DWARF proteins from tomato (64% identity and 89% similarity) (Bishop *et al.*, 1996) and C-6 oxidase from *Arabidopsis* (58% identity and 88% similarity) (Shimada *et al.*, 2001)

Figure 6. Phenotypic rescue of the abnormal morphology of *brd1* by exogenous BL treatment. The wild-type (wt) and *brd1-1* plants grown in soil for 4 weeks were treated with 10^{-6} M BL solution (+) or water (–) from the beginning of germination (bar: 10 cm).

over almost the entire region (Figure 7a). These proteins have been categorized into the family of cytochromes P450 (P450s); there are numerous members of this family in higher plants with high structural similarity. To determine whether our rice candidate protein can be classified into the DWARF protein group (CYP85 group), we compared the sequence similarity of the candidate with other members of P450, such as CYP90 groups (CPD, DWF4, and ROT3) and CYP88 (kaurenic acid oxidase). These proteins are involved in either BR biosynthesis (DWARF, CPD, DWF4), GA biosynthesis (kaurenic acid oxidase), or have an unknown function (ROT3) (Figure 7b). The phylogenic relationship calculated by the neighbor joining method demonstrated that OsDWARF can be classified into the same group as the tomato and *Arabidopsis* DWARF proteins, and it is designated CYP85A1 according to the nomenclature of the P450 superfamily (Nelson *et al.*, 1996). These comparative studies strongly suggest that OsDWARF is a member of the DWARF proteins.

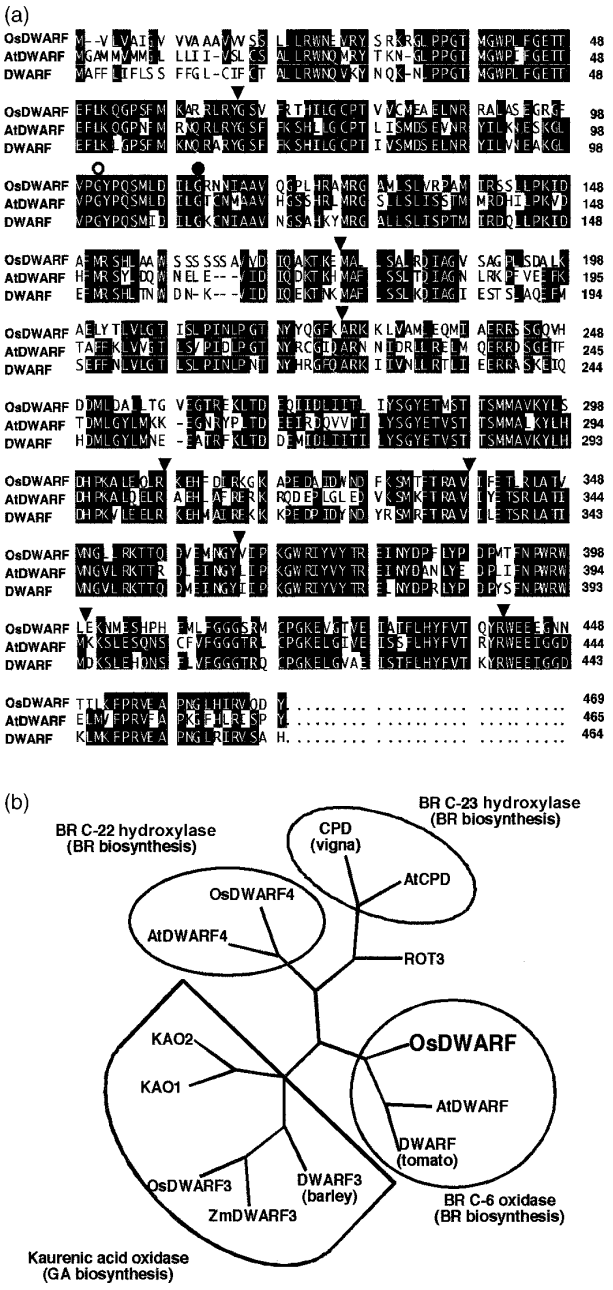

Figure 7. Structure of the *OsDWARF* gene.
(a) Alignment of the deduced amino acid sequences of the *DWARF* genes from rice, *Arabidopsis*, and tomato. Dashes (–) indicate gaps introduced to maximize alignment. Identical amino acid residues are represented by white-on-black letters. Filled triangles indicate the positions of intron sites in the *OsDWARF* gene. Filled and open circles show the substituted amino acids in *brd1-2* and *brd1-3*, respectively. The GenBank/EMBL/DDBJ accession numbers of the *OsDWARF*, *AtDWARF*, and *DWARF* are AB084385, AB035868, and U54770, respectively.
(b) Phylogenetic relationship between the *OsDWARF* gene and other P450 genes in plants using the neighbor-joining method. The selected plant P450 genes are classified into two groups, that is, BR biosynthesis and GA biosynthesis, except ROT3. Accession numbers: AtCPD (X87367), AtDWARF (AB035868), AtDWARF4 (AF044216), CPD vigna (AF279252), DWARF tomato (U54770), DWARF3 barley (AF326277), KAO1 (AF318500), KAO2 (AF318501), OsDWARF (AB084385), OsDWARF3 (BAA85446), OsDWARF4 (Sakamoto and Matsuoka, unpublished data), ROT3 (AB008097), ZmDWARF3 (U32579).

Table 1 C-6 oxidation of BRs by OsDWARF expressed in yeast

Substrate	Product	Conversion rate[a]
[$^2H_6$]6-DeoxoCS	[$^2H_6$]CS	13
[$^2H_6$]6-DeoxoCS	[$^2H_6$]6-OHCS	6
[$^2H_6$]6-DeoxoTY	[$^2H_6$]TY	30
[$^2H_6$]6-Deoxo3DT	[$^2H_6$]3DT	22
[$^2H_6$]6-DeoxoTE	[$^2H_6$]TE	20
[$^2H_6$]6-DeoxoCT	[$^2H_6$]CT	nd[b]
[$^2H_6$]CN	[$^2H_6$]6-OxoCN	nd

[a]The conversion rate was calculated as a percentage of the amount of each metabolite versus the amount of substrate added to the culture.
[b]Not detected.

The sequence similarity between OsDWARF and the previously reported DWARF proteins does not directly mean that the rice protein has C-6 oxidase activity. To establish the biochemical function of OsDWARF, the cDNA fragment was subcloned into a yeast expression vector and expressed in the yeast strain WAT11, which carries a clone for *Arabidopsis* NADPH-P450 reductase (Urban *et al*., 1997). In this strain, the expression of both OsDWARF and P450 reductase is induced by treatment with Galactose (Gal) (Pompon *et al*., 1996). We incubated deuterated BRs with the Gal-treated yeast culture and analyzed the products of the reaction by GC–MS. The conversion rate from the deuterated substrate to each product is summarized in Table 1. When [$^2H_6$]6-DeoxoCS was fed to the yeast strain expressing OsDWARF, both [$^2H_6$]CS and [$^2H_6$]6α-hydroxycastasterone (6-OHCS) were identified as metabolites, whereas BL was not identified in the reaction mixture (Table 1). This result confirms the C-6 oxidase activity of OsDWARF in the yeast cells.

Since the accumulation profile of the intermediate BRs in the mutants indicated that OsDWARF may have C-6 oxidase activity for other 6-DeoxoBRs (Figure 5), we further investigated the activity of the OsDWARF protein. The protein converted [$^2H_6$]6-DeoxoTY, [$^2H_6$]3-dehydro-6-deoxoteasterone (6-Deoxo3DT) and [$^2H_6$]6-DeoxoTE to [$^2H_6$]TY, [$^2H_6$]3-dehydroteasterone (3DT) and [$^2H_6$]TE, respectively, whereas [$^2H_6$]6-DeoxoCT and [$^2H_6$]CN were not converted by the protein. The substrate specificity of OsDWARF in yeast cells corresponds to the accumulation pattern of the BRs, and therefore OsDWARF in rice should have the same activity as that observed in yeast cells.

Characterization of loss-of-function alleles in brd1 *mutants and molecular complementation of the* brd1 *mutation by introduction of the* OsDWARF *gene*

We compared the sequence of *OsDWARF* in the mutants with that of the wild-type, and identified a single nucleotide substitution or nucleotide deletions in each *brd1* mutant allele (Figure 8a). The *brd1-1* allele had a 113 nucleotide deletion from the 5′-side of intron 6 to the 5′-side of exon 7. This nucleotide deletion created a novel stop codon just downstream of the deletion point and consequently this mutant allele should produce a truncated protein without the heme-binding site. Because the heme-binding site is essential for the activity of P450, this allele should be functionally null. In fact, the *brd1-1* plants had the severe phenotype. The mutation in *brd1-2* was a single nucleotide substitution to exchange glycine with valine at residue 111. This glycine residue is conserved among all members of CYP85, CYP90 and CYP88 (data not shown), indicating that it is important for the expression of the enzymatic activity. Actually, *brd1-2* showed a severe phenotype similar to that of *brd1-1*. The mutation in *brd1-3* was a single nucleotide substitution to exchange glycine with valine at residue 101. This residue is conserved among the three DWARF proteins but not among the related P450 members. Correspondingly, the phenotype of *brd1-3* was the least severe of the three mutant alleles.

To confirm that the *OsDWARF* gene corresponds to the *brd1* locus, we performed a complementation experiment

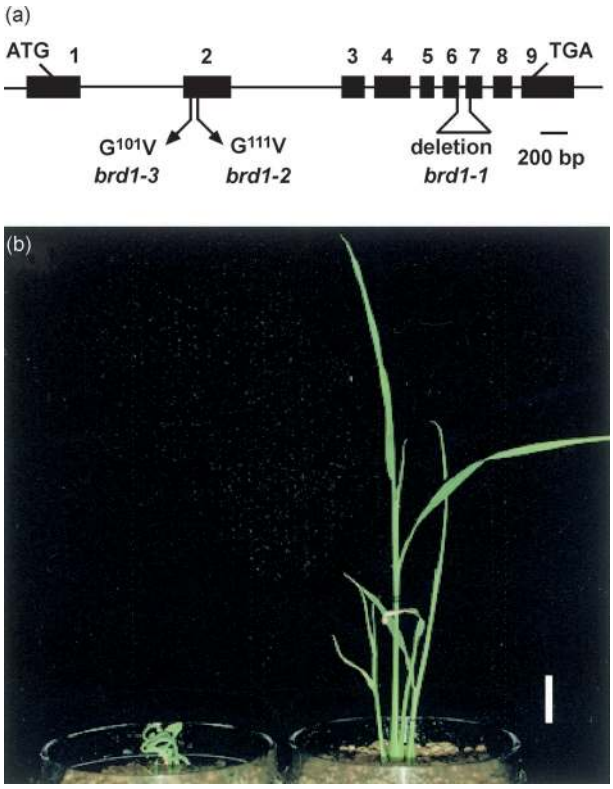

Figure 8. Complementation of the *brd1* phenotype by introduction of *OsDWARF*.
(a) Genomic structure of *OsDWARF* and position of mutations in the *brd1* alleles. Black boxes represent exons.
(b) The *brd1-1* mutant containing the vector only (left) and the DNA fragment encompassing the entire *OsDWARF* gene (right) (bar: 1 cm).

using the *brd1-1* mutant. Transformation with a control vector that contained no insert had no apparent effect on the abnormal phenotype (plant to the left in Figure 8b). However, when a 8.5-kb DNA fragment containing the entire gene was introduced, the normal phenotype was recovered in almost all of the plants that were resistant to a selection marker for transformation, hygromycin (the plant to the right in Figure 8b). This result confirms that the *brd1* mutation is caused by the loss-of-function of the *OsDWARF* gene.

Expression analyses of OsDWARF *gene*

There are no data on the site of synthesis of the bioactive BRs in monocot plants. Therefore, we examined the expression pattern of the *OsDWARF* gene in various rice organs. RNA gel blot analysis using the entire length of the cDNA fragment for *OsDWARF* as a probe did not result in any bands that hybridized with the probe, so we performed a semi-quantitative reverse-transcription PCR (RT–PCR) analysis to estimate the level of the *OsDWARF* transcript. RNA extracted from the leaf sheath produced the strongest band (Figure 9a). Bands with intermediate intensity were amplified with RNAs from the stem and elongating stem, while the RNAs from the root, flower, rachis and SAM produced only faint bands. The preferential expression of *OsDWARF* in the leaf sheath and elongating stem corresponds to the severe abnormal phenotype of the leaf sheath and internode. Thus, it is possible that the biosynthesis of active BRs occurs primarily in the developing leaf sheath and elongating stem.

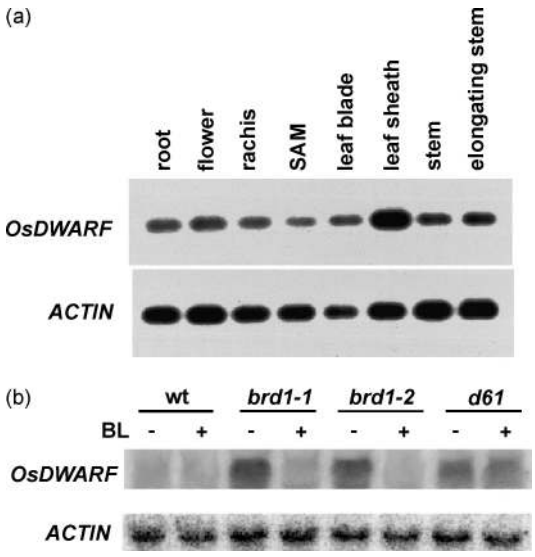

Figure 9. Expression pattern of the *OsDWARF* gene in various organs and the negative feedback effect of BL on *OsDWARF* expression.
(a) Organ specific expression of the *OsDWARF* gene in the wild-type plant. Total RNAs were isolated from various organs indicated at top, and RT-PCR was conducted. Signals were detected with the ^{32}P-labeled cDNA clone indicated at left. Expression of the *Actin* gene was used as a control.
(b) Negative feedback regulation of the *OsDWARF* gene by BL. Total RNAs were prepared from seedlings of the wild-type, *brd1-1*, *brd1-2*, and *d61* with or without exogenous application of BL (10^{-6} M). The RNAs were blotted into nylon membranes, and the membranes were probed with ^{32}P-labeled *OsDWARF* cDNA. The bottom panel shows the *Actin* probe as a control.

We also studied the effect of BL on *OsDWARF* expression. A higher level of *OsDWARF* expression was detected in the *brd1* mutants compared to the wild-type plants (Figure 9b). However, the expression of *OsDWARF* in the mutants was dramatically reduced by treatment with BL. A higher level of *OsDWARF* expression was also seen in *d61-2*, which is partially defective in the BR signaling pathway (Yamamuro *et al.*, 2000). In *d61-2*, the exogenous BL treatment did not alter *OsDWARF* expression as effectively as it did in the *brd1* mutants (Figure 9b). These results indicate that the expression of *OsDWARF* is negatively regulated by the BR signal transduction pathway.

Discussion

This study describes the isolation and characterization of BR-deficient mutants of rice, *brd1*. This is the first report to describe the phenotypic characterization of a BR-deficient mutant in monocot plants. On the basis of the following observations, we have concluded that the abnormal phenotypes of the *brd1* mutants are caused by a defect in BR biosynthesis. First, the level of the active BR (CS) in rice was dramatically reduced in the mutant plants (Figure 5). Secondly, the exogenous application of BL restored the abnormal morphology of the leaves of the *brd1* mutants (Figure 6). Finally, the *BRD1* gene encodes a protein that catalyzes the C-6 oxidation step in BR synthesis (Table 1).

The OsDWARF protein and BR metabolism in rice

We could not detect BL, the most bioactive BR, in seedlings of the mutants or the wild-type plants, and it is possible that CS is the dominant bioactive BR in rice. In fact, BL was not detected even in the rice BR-insensitive mutant *d61*, which contains a higher level of BRs (including CS) than wild-type plants because it actively synthesizes BRs in a homeostatic manner under the diminished sensitivity to BRs (Yamamuro *et al.*, 2000). The conversion from 6-DeoxoCS to CS causes a 200-fold increase in the bioactivity of BRs (Fujioka *et al.*, 1998), and when CS is dominant among the active BRs in rice, the reaction catalyzed by the OsDWARF protein is the last step to produce bioactive BR. The expression pattern of the *OsDWARF* gene, therefore should reflect the location of active BR production in rice plants, and mutants deficient in OsDWARF activity should show the typical severe BR-deficient phenotype.

In yeast cells, the OsDWARF protein catalyzed multiple reaction steps in BR biosynthesis, that is, 6-DeoxoTE to TE, 6-Deoxo3DT to 3DT, 6-DeoxoTY to TY, and 6-DeoxoCS

to CS (Table 1). This is consistent with the levels of some BRs detected in *brd1*. Actually, the levels of 6-DeoxoTE, 6-DeoxoTY and 6-DeoxoCS were increased in the mutants compared to the wild-type, whereas the levels of TE, TY, and CS were decreased (Figure 5). Taken together, these results suggest that the OsDWARF protein actively catalyzes the C-6 oxidation of multiple substrates in plants. Differences in C-6 oxidation activity in yeast cells and in *planta* have been reported previously (Shimada *et al.*, 2001). In tomato, for example, no BR compounds in the early C-6 oxidation pathway were detected except CS (Bishop *et al.*, 1999), even though the enzyme catalyzed the C-6 oxidation of 6-DeoxoTE, 6-Deoxo3DT, 6-DeoxoTY and 6-DeoxoCS in yeast (Shimada *et al.*, 2001). Similarly, the *Arabidopsis* C-6 oxidase catalyzed multiple reactions in yeast (Shimada *et al.*, 2001), despite the fact that neither 3DT nor TE could be recovered from 6-Deoxo3DT or 6-DeoxoTE in *Arabidopsis* plants exposed to deuterium-labeled BRs (Noguchi *et al.*, 2000). Shimada *et al.* (2001) suggest that these differences may be owing to either the rapid turn-over of 6-Oxo BRs, such as TE and TY, in plants, or a very slow metabolic flow from 6-DeoxoTE to TE and 6-Deoxo3DT to 3DT. Our results strongly support the former possibility. The inability to detect the reaction steps from 6-DeoxoTE to TE, and 6-Deoxo3DT to 3DT, in *Arabidopsis* may be owing to the rapid metabolism of these 6-Oxo BRs to TY or CS.

The exogenous application of BL to *brd1-1* restored the abnormal morphology of the leaves but did not completely restore the height of the plants (Figure 6). The partial restoration of the dwarf phenotype of *brd1-1* may be owing to the poor incorporation of the exogenously applied BL into the rice plants. A similar phenomenon has been observed in the tomato BR-deficient mutant *extreme dwarf* (Bishop *et al.*, 1999). Treatment of the tomato mutant with BL effectively restored the dwarf phenotype but the length of hypocotyl did not reach that of the wild-type tomato. To explain this partial restoration of dwarfism in mutant tomato plants, Bishop *et al.* (1999) hypothesized that the increased level of 6-DeoxoCS in the mutant may act as a competitive inhibitor of the BR receptor and thus could prevent or reduce signaling for the downstream responses. Since rice has an OsBRI1 protein with a very similar structure to the *Arabidopsis* BRI1 (Yamamuro *et al.*, 2000), it is possible that there may be a similar mechanism in rice plants.

BRs are essential for the organized arrangement and polar elongation of cells in the leaf and stem

The defect in BR biosynthesis induced a wide range of abnormalities in organ development and growth, the most remarkable of which were changes in the shape and arrangement of cells in the internode and leaf epidermis. In plant cells, the cortical microtubules are arranged transversely to the cell axis and determine the orientation of cellulose microfibrils in the cell wall, thereby controlling the shape of plant cells and the direction of cell expansion. Munoz *et al.* (1998) demonstrated that BL-induced growth in chickpea epicotyls is accompanied by the increased expression of the β-tubulin gene. Conversely, in the *Arabidopsis* BR-deficient mutant, *dim*/*dwarf1*, the expression of the β-tubulin gene is suppressed and this inhibits the elongation of hypocotyl cells (Takahashi *et al.*, 1995). Since microtubules are primarily composed of α- and β-tubulin polypeptides, decreased expression of the β-tubulin gene will seriously damage the formation of cortical microtubules, and consequently will affect cell shape. It is possible that the abnormal shape of the leaf surface cells in the *brd1* mutants may be owing to a failure in cortical microtubule formation caused by the decreased expression of the β-tubulin gene in response to low BR levels.

It has also been reported that BRs promote the transverse arrangement of cortical microtubules to accelerate cell elongation (Mayumi and Shibaoka, 1995). Therefore, the decreased level of BRs should affect not only microtubule formation but also the transverse arrangement of microtubules. In a previous study of the microtubules in internode cells of *d61*, we could not detect microtubules in unelongated internode cells and found that the microtubules in elongating internode cells were disorganized, whereas the microtubules in elongating internode cells of the wild-type plants were arranged in an orderly manner at right angles to direction of elongation (Yamamuro *et al.*, 2000). These observations indicate that the internode cells of the *brd1* mutants also have a failure in microtubule formation and microtubule arrangement, since the shape and arrangement of the *brd1* internode cells was essentially the same as that of the unelongated internode of *d61*. It is important to distinguish between the deficiency in microtubule formation and microtubule arrangement when considering the biological function of BRs. In fact, the GA-deficient dwarf mutant *d18*, which retains normal microtubule formation but not correct microtubule arrangement, shows an inhibition of leaf surface cell elongation but not aberrant cell shape or cell files (Ueguchi-Tanaka *et al.*, unpublished data). In this context, the malformed cell shape observed in the leaf surface of the *brd1* mutants is a typical characteristic of the BR-related phenotype.

Another remarkable phenotype of the *brd1* mutants is the disorganization of the cell files in the leaf epidermis and internodes, and the disorganized layer of bundle sheath cells in the vascular tissues. The disruption of the cell files or layers is caused by an incorrect determination of the cell division site. The pre-prophase band (PPB) of microtubules and phragmoplast play important roles in determining the site of cell division and formation of the new cell plate, respectively. The PPB arises as cortical microtubules gather at a specific site in the cell that precisely predicts the plane

of subsequent cytokinesis, and the phragmoplast is also mainly composed of microtubules and actin filaments (Pickett-Heaps *et al.*, 1999). Therefore, the reduction of BR levels in the mutants may affect the formation of the PPB and phragmoplast through the decreased expression of β-tubulin, resulting in the loss of determination of the cell division site. Taken together, these findings indicate that the malformed cell shape and aberrant cell files observed in the *brd1* mutants may be associated with a defect in the formation and arrangement of microtubules. Therefore, it is possible that BRs control organ development and growth by regulating the formation and arrangement of microtubules in actively proliferating and elongating cells.

Feedback regulation of OsDWARF *expression by BL*

It is well recognized that GA biosynthesis is controlled by the level of active GAs in a feedback manner through the regulation of the expression of GA biosynthesis genes such as GA20 oxidase and GA3 oxidase, both of which catalyze late steps in the GA biosynthetic pathway. By analogy with GA biosynthesis, we predicted that the *OsDWARF* gene, whose product catalyzes a late step in bioactive BR synthesis, might be negatively regulated by bioactive BRs. The expression profile of *OsDWARF* confirmed this, clearly demonstrating that *OsDWARF* expression is regulated by the level of the bioactive BR, BL (Figure 9b). The partial suppression observed in *d61* following BL treatment may be owing to the fact that the mutant retains some BR-signaling activity. In fact, the phenotype of *d61-2*, the severest allele of *d61,* was much milder than that of *brd1-1* or *brd1-2*, and *d61-2* still responded to the exogenously applied BL to stimulate lamina inclination (Yamamuro *et al.*, 2000). Mathur *et al.* (1998) reported a similar phenomenon in which *CPD* expression is negatively regulated by exogenous BR treatment. Although there are no reports describing the negative regulation of genes for BR biosynthetic enzymes in other plants, our recent observations demonstrate that the expression of rice genes homologous to *Arabidopsis CPD* and *DWF4* is also downregulated by treatment with BL (Hong *et al.*, unpublished data). Since the product of the *CPD* gene catalyzes the conversion of CT and 6-DeoxoCT to TE and 6-DeoxoTE, respectively, at least a few enzymes from the steps catalyzed by CPD may be involved in BR biosynthesis to produce bioactive BRs. It will be interesting to determine if the expression of genes that encode the enzymes catalyzing the steps from CPD to DWARF are also negatively regulated by active BR levels, as occurs for *DWF4*, *CPD* and *OsDWARF*. Whether the mechanism(s) involved in the negative feedback regulation of BRs is the same or different for each gene also remains to be determined. Clearly, further studies are needed to investigate the molecular mechanism of BR biosynthesis.

Experimental procedures

Plant materials and growth conditions

Wild-type rice plants (*Oryza sativa* cv. Nipponbare), three mutant alleles of *brd1*, BR-insensitive mutant of *d61* (Yamamuro *et al.*, 2000), and GA-deficient mutant of *d18 (*Itoh *et al.*, 2001) were grown in a greenhouse at 30°C (day) and 24°C (night). All of the three alleles of *brd1* were from Nipponbare, which were derived from regenerated rice plants after cell suspension culture for several months.

Microscopic analyses

For light microscopy, tissues were fixed in formaldehyde:glacial acetic acid:70% ethanol (1 : 1 : 18 [v:v:v]) and dehydrated in a graded ethanol series. The samples were embedded in Paraplast Plus (Sherwood Medical, St. Louis, MO). Microtome sections of 10 μm thickness were applied to silan-coated glass slides (Matsunami Glass, Osaka, Japan). The sections were de-paraffinized in xylene, dehydrated through a graded ethanol series, and dried overnight before staining with toluidine blue. For SEM, fixed and unfixed leaves were observed using a S-3000H scanning electron microscope (HITACHI, Tokyo, Japan). Fixation was performed by the same methods described above.

Quantification of endogenous BRs

Shoots from wild-type and mutant plants were harvested at 6 weeks after germination and lyophilized immediately at −80°C. Lyophilized shoots (equivalent to 20 g fresh weight) were extracted twice with 250 ml of methanol:$CHCl_3$ (4 : 1 [v:v]), and deuterium-labeled internal standards 1 ng/g fresh weight) were added. Purification and (GC–MS) analyses were performed as described in Noguchi *et al.* (1999).

Yeast functional assay

OsDWARF cDNA was amplified using primers containing the *Bam*HI and *Eco*RI sites (5′-GGCGGATCCATGGTGTTGGTGGC-GATTG-3′ and 5′-GCCGAATTCCTACCATCTGTATTGAGTC-3′). The amplified fragment was fully sequenced. The fragment was digested with *Bam*HI and *Eco*RI and ligated into a pYeDP60 vector for expression in yeast. The *OsDWARF* fragment in the pYeDP60 vector was transformed into the yeast strain WAT11. Purification and GC–MS analyses were performed as described in Noguchi *et al.* (1999).

Exogenous BL treatment

Rice seeds were imbibed in BL solution (10^{-6} M) for 3 days and then grown in soil containing BL (10^{-6} M) for 4 weeks.

Isolation, sequencing and mapping of the OsDWARF gene

We identified a rice EST clone (AU100843) in the rice database based on its high sequence similarity to the tomato *DWARF* gene. The EST clone was used to probe a rice seed cDNA library to isolate the full-length cDNA encoding *OsDWARF*. The longest cDNA (1933 bp) was sequenced by the dideoxy chain termination method

using an automatic DNA sequencer (ABI PRISM 310–10, Applied Biosystems, Foster City, CA, USA) according to the manufacturer's instructions. Both strands were entirely sequenced. To identify the mutation sites of the three alleles, we amplified the *OsDWARF* gene using the genomic DNA extracted from the three mutants. The amplified DNA fragments were directly sequenced with appropriate primers without cloning. To isolate a genomic *OsDWARF* clone, we performed PCR screening of the BAC library produced in Clemson University Genomics Institute (CS, USA) using a set of primers (5′-CACAACCTCATACAGAAGG-3′ and 5′-CGCATGATGCAGAGATTGC-3′). An XBH01–2F12 clone containing the entire genomic *OsDWARF* clone was digested with *Not*I and *Bam*HI, and ligated into a pBluescript vector (Stratagene, La Jolla, CA, USA). For mapping of the *brd1* mutant, F_2 populations derived from the cross between heterozygous plant for *brd1* and indica variety, Kasalath, were analyzed (Lin *et al.*, 1998). One hundred plants homozygous recessive for *brd1* were screened with molecular markers for linkage analysis (Harushima *et al.*, 1998).

Complementation of the brd1 *mutant*

A genomic *OsDWARF* clone in a pBluescript vector was digested with *Not*I and *Bam*HI, and filled into blunt ends. The fragment (8.5 kb) was inserted at the *Sma*I site of the hygromycin-resistance binary vector pBI-Hm12, which was kindly provided by Dr Hiroyuki Hirano (Tokyo University, Tokyo). The construct was introduced into *brd1-1* by *Agrobacterium tumefaciens*-mediated transformation, as described by Hiei *et al.* (1994). Control plants were transformed with the pBI-Hm12 vector.

RNA analyses

RNA was isolated from various rice tissues by the standard SDS–phenol method, and treated with *DNase*I. The 1st strand cDNAs were synthesized from 1 μg total RNA using an Omniscript RT kit (Qiagen, Hilden, Germany). The cDNAs were amplified with the primers 5′-GGAGAAGAACATGGAATCAC-3′ and 5′-GTAATCTTGAACGCGGATATG-3′, located at exon 8 and 9, respectively. The amplified products were separated on a 1% agarose gel and blotted onto a Hybond N+ membrane (Amersham Pharmacia, Piscataway, NJ, USA). The membrane was hybridized with the ^{32}P-labeled cDNA. The conditions of hybridization were the same as those given for screening of the cDNA. A Fuji Imaging Plate was exposed to the membranes and the image was visualized using a BAS2000 Imaging Analyzer (Fuji Photo Film Co., Tokyo, Japan). As a control, we amplified the rice actin1 transcript with the primers 5′-TCCATCTTGGCATCTCTCAG-3′ and 5′-GTACCCGCATCAGGCATCTG-3′, and detected the amplified fragment by its ^{32}P-labeled cDNA.

Rice seeds were germinated in MS medium in the presence or absence of 10^{-6} M BL. After 2 weeks of germination, total RNA was isolated by the standard SDS–phenol method. Total RNA (7.5 μg) was separated on a 1% agarose gel, transferred to a Hybond N+ membrane, and hybridized with ^{32}P-labeled cDNA. The conditions were the same as those given for the screening of cDNA.

Acknowledgements

We are grateful to Dr Kazumi Hattori (Nagoya University, Nagoya, Japan) for his excellent help with SEM. We also thank Ms. Masayo Sekimoto (RIKEN, Saitama, Japan), Mr Makoto Kobayashi (RIKEN, Saitama, Japan), and Ms. Masako Hattori (Nagoya University, Nagoya, Japan) for technical assistance. This work was supported in part by a Grant-in-Aid from the Program for the Promotion of Basic Research Activities for Innovative Biosciences (M. M., M. U.-T. and S. S.-S.) and Grant-in-Aid for Center of Excellence (M. M. and Y. I.).

References

Ashikari, M., Wu, J., Yano, M., Sasaki, T. and Yoshimura, A. (1999) Rice gibberellin-insensitive dwarf mutant gene *Dwarf1* encodes the α-subunit of GTP-binding protein. *Proc. Natl Acad. Sci. USA*, **96**, 10284–10289.

Bishop, G.J., Harrison, K. and Jones, J.D.G. (1996) The tomato *Dwarf* gene isolated by heterologous transposon tagging encodes the first member of a new cytochrome P450 family. *Plant Cell*, **8**, 959–969.

Bishop, G.J., Nomura, T., Yokota, T., Harrison, K., Noguchi, T., Fujioka, S., Takatsuto, S., Jones, J.D.G. and Kamiya, Y. (1999) The tomato DWARF enzyme catalyses C-6 oxidation in brassinosteroid biosynthesis. *Proc. Natl Acad. Sci. USA*, **96**, 1761–1766.

Choe, S., Dilkes, B.P., Fujioka, S., Takatsuto, S., Sakurai, A. and Feldmann, K.A. (1998) The *DWF4* gene of *Arabidopsis* encodes a cytochrome P450 that mediates multiple 22α-hydroxylation steps in brassinosteroid biosynthesis. *Plant Cell*, **10**, 231–243.

Clouse, S.D. and Sasse, J.M. (1998) Brassinosteroids: essential regulators of plant growth and development. *Annu. Rev. Plant Physiol. Plant Mol. Biol.* **49**, 427–451.

Clouse, S.D. and Zurek, D. (1991) Molecular analysis of brassinolide action in plant growth and development. In: *Brassinosteroids: Chemistry, Bioactivity and Applications* (Yokota, T. and Adam, G., eds). Washington, DC: American Chemical Society, pp. 122–140.

Evans, L.T. (1993) *Crop Evolution, Adaptation and Yield. Cambridge*. Cambridge University.

Fujioka, S., Noguchi, T., Yokota, T., Takatsuto, S. and Yoshida, S. (1998) Brassinosteroids in *Arabidopsis thaliana*. *Phytochemistry*, **48**, 595–599.

Gale, M.D. and Youssefian, S. (1985) *Progress in plant breeding* (Russell, G.E., ed.). London: Butterworth, pp. 1–35.

Harushima, Y., Yano, M., Shomura, A. *et al.* (1998) A high-density rice genetic linkage map with 2275 markers using a single F_2 population. *Genetics*, **148**, 479–494.

Hiei, Y., Ohta, S., Komari, T. and Kumashiro, T. (1994) Efficient transformation of rice (*Oryza Sativa* L.) mediated by *Agrobacterium* and sequence analysis of the boundaries of the T-DNA. *Plant J.* **6**, 270–282.

Itoh, H., Ueguchi-Tanaka, M., Sato, Y., Ashikari, M. and Matsuoka, M. (2002) The gibberellin signaling pathway is regulated by the appearance and disappearance of SLENDER RICE1 in nuclei. *Plant Cell*, **14**, 57–70.

Itoh, H., Ueguchi-Tanaka, M., Sentoku, N., Kitano, H. and Matsuoka, M. (2001) Cloning and functional analysis of two gibberellin 3β-hydroxylase genes that are differently expressed during the growth of rice. *Proc. Natl Acad. Sci. USA*, **98**, 8909–8914.

Iwasaki, T. and Shibaoka, H. (1991) Brassinosteroids act as regulators of tracheary-element differentiation in isolated *Zinnia* mesophyll cells. *Plant Cell Physiol.* **32**, 1007–1014.

Lin, S.Y., Sasaki, Y. and Yano, M. (1998) Mapping quantitative trait loci controlling seed dormancy and heading date in rice, *Oryza sativa* L. using backcross inbred lines. *Theor. Appl. Genet.* **96**, 997–1003.

Maeda, E. (1965) Rate of lamina inclination in excised rice leaves. *Physiol. Plant.* **18**, 813–827.

Mathur, J., Molnar, G., Fujioka, S. *et al.* (1998) Transcription of the *Arabidopsis CPD* gene, encoding a steroidogenic cytochrome P450, is negatively controlled by brassinosteroids. *Plant J.* **14**, 593–602.

Mayumi, K. and Shibaoka, H. (1995) A possible double role for brassinolide in the reorientation of cortical microtubules in the epidermal cells of azuki bean epicotyls. *Plant Cell Physiol.* **36**, 173–181.

Munoz, F.J., Labrador, E. and Dopico, B. (1998) Brassinolides promote the expression of a new *Cicer arietinum* β-tubulin gene involved in the epicotyl elongation. *Plant Mol. Biol.* **37**, 807–817.

Nakaya, M., Tsukaya, H., Murakami, N. and Kato, M. (2002) Brassinosteroids control the proliferation of leaf cells of *Arabidopsis thaliana*. *Plant Cell Physiol.* **43**, 239–244.

Nelson, D.R., Koymans, L., Kamataki, T. *et al.* (1996) P450 superfamily: update on new sequences, gene mapping, accession numbers and nomenclature. *Pharmacogenetics* **6**, 1–42.

Noguchi, T., Fujioka, S., Choe, S., Takatsuto, S., Tax, F.E., Yoshida, S. and Feldmann, K.A. (2000) Biosynthetic pathway of brassinolide in *Arabidopsis*. *Plant Physiol.* **124**, 201–209.

Noguchi, T., Fujioka, S., Takatsuto, S., Sakurai, A., Yoshida, S., Li, J. and Chory, J. (1999) *Arabidopsis det2* is defective in the conversion of (24*R*)-24-methylcholest-4-en-3-one to (24*R*)-24-methyl-5α-cholestan-3-one in brassinosteroid biosynthesis. *Plant Physiol.* **120**, 833–839.

Pickett-Heaps, J.D., Gunning, B.E.S., Brown, R.C., Lemmon, B.E. and Cleary, A.L. (1999) The cytoplast concept in dividing plant cells: cytoplasmic domains and the evolution of spatially organized cell division. *Am. J. Bot.* **86**, 153–172.

Pompon, D., Louerat, B., Bronine, A. and Urban, P. (1996) Yeast expression of animal and plant P450s in optimized redox environments. *Meth. Enzymol.* **272**, 51–64.

Sasaki, A., Ashikari, M., Ueguchi-Tanaka, M. *et al.* (2002) A mutant gibberellin-synthesis gene in rice. *Nature*, **416**, 701–702.

Sasse, J. (1999) Physiological actions of brassinosteroids. In: *Brassinosteroids: Steroidal Plant Hormones* (Sakurai, A., Yokota, T. and Clouse, S.D., eds). Tokyo: Springer–Verlag, pp. 137–161.

Shimada, Y., Fujioka, S., Miyauchi, N., Kushiro, M., Takatsuto, S., Nomura, T., Yokota, T., Kamiya, Y., Bishop, G.J. and Yoshida, S. (2001) Brassinosteroid-6-oxidases from *Arabidopsis* and tomato catalyze multiple C-6 oxidations in brassinosteroid biosynthesis. *Plant Physiol.* **126**, 770–779.

Szekeres, M., Nemeth, K., Koncz-Kalman, Z., Mathur, J., Kauschmann, A., Altmann, T., Redei, G.P., Nagy, F., Schell, J. and Koncz, C. (1996) Brassinosteroids rescue the deficiency of CYP90, a cytochrome P450, controlling cell elongation and deetiolation in *Arabidopsis*. *Cell*, **85**, 171–182.

Takahashi, T., Gasch, A., Nishizawa, N. and Chua, N.H. (1995) The *DIMINUTO* gene of *Arabidopsis* is involved in regulating cell elongation. *Genes Dev.* **9**, 97–107.

Takeno, K. and Pharis, R.P. (1982) Brassinosteroid-induced bending of the leaf lamina of dwarf rice seedlings: an auxin-mediated phenomenon. *Plant Cell Physiol.* **23**, 1275–1281.

Ueguchi-Tanaka, M., Fujisawa, Y., Kobayashi, M., Ashikari, M., Iwasaki, Y., Kitano. H. and Matsuoka, M. (2000) Rice dwarf mutant *d1*, which is defective in the α subunit of the heterotrimeric G protein, affects gibberellin signal transduction. *Proc. Natl Acad. Sci. USA*, **97**, 11638–11643.

Urban, P., Mignotte, C., Kazmaier, M., Delorme, F. and Pompon, D. (1997) Cloning, yeast expression and characterization of the coupling of two distantly related *Arabidopsis thaliana* NADPH-cytochrome P450 reductases with P450 CYP73A5. *J. Biol. Chem.* **272**, 19176–19186.

Wada, K., Kondo, H. and Marumo, S. (1985) A simple bioassay for brassinolides: a wheat leaf-unrolling test. *Agric. Biol. Chem.* **49**, 2249–2251.

Wada, K., Marumo, S., Ikekawa, N., Morisaki, M. and Mori, K. (1981) Brassinolide and homobrassinolide promotion of lamina inclination of rice seedlings. *Plant Cell Physiol.* **22**, 323–325.

Yamamuro, C., Ihara, Y., Wu, X., Noguchi, T., Fujioka, S., Takatsuto, S., Ashikari, M., Kitano, H. and Matsuoka, M. (2000) Loss of function of a rice *brassinosteroid insensitive1* homolog prevents internode elongation and bending of the lamina joint. *Plant Cell*, **12**, 1591–1605.

Accession number: OsDWARF (AB084385).